The neuron

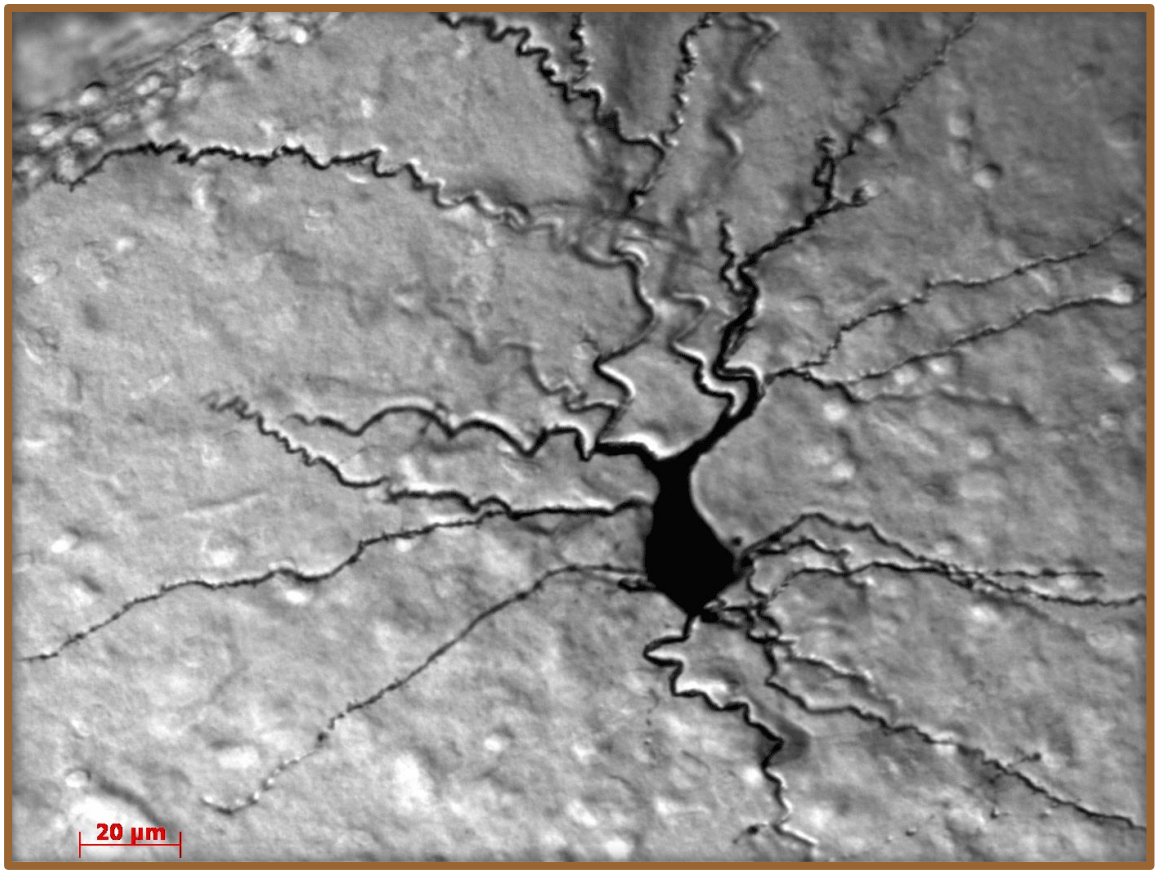

Biocytin labeled pyramidal neuron recorded in piriform cortex

Discovery of the neuron

The Nobel Prize in Physiology or Medicine 1906

"in recognition of their work on the structure of the nervous system"

New invention:

- the silver impregnation technique (Golgi stainining)

Camillo Golgi

Pavia University
Pavia, Italy

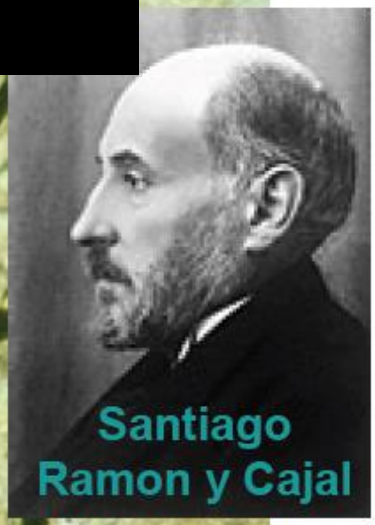

Santiago Ramon y Cajal

Madrid University
Madrid, Spain

(A) Reticularist Doctrine

(B) Neuron Doctrine ⟸ winner

In retrospect, it is clear that one reason for the long confusion over this issue (discrete cells or a continuous syncytium) is the complexity of brain tissue…

A large number of different neuron types exist and many of them have a complex asymmetric, 3D-structure that makes it extremely difficult to ascertain where one cell ends and the next begins

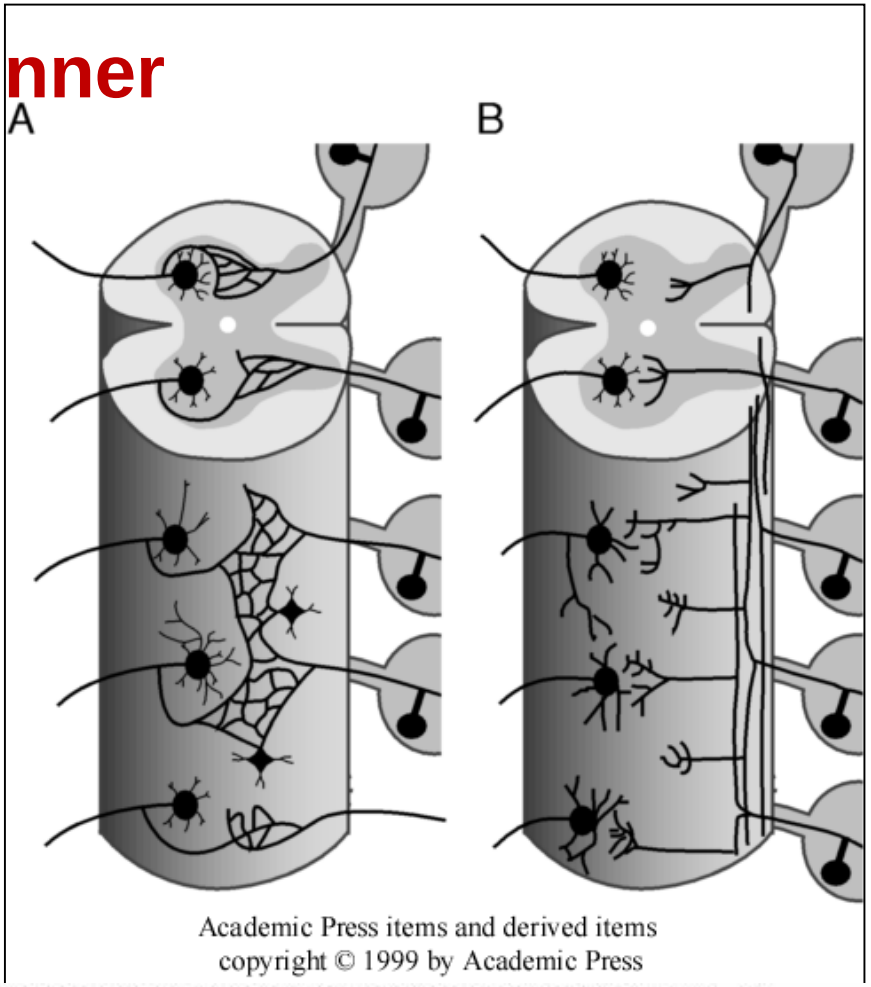

FIGURE 2 The nervous system is a reticulum versus the neuron doctrine. (A) Proponents of the reticularist's view of the nervous system believed that neurons are physically connected to one another, forming an uninterrupted network. (B) The neuron doctrine, in contrast, considers each neuron an individual entity that communicates with target cells across an appropriate intercellular gap. Adapted from Cajal (1911–1913).

Exception to Neuron Doctrine……

….GAP JUNCTIONS between neurons

Studying the unique structure of neurons: cells devoted to “information transfer”, both intracellularly and intercellularly

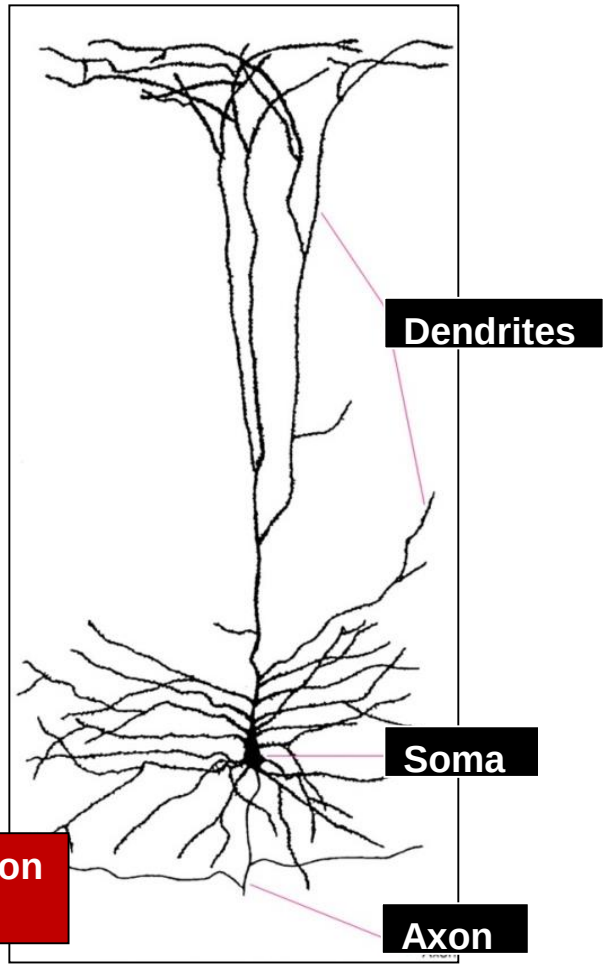

Pyramidal neuron (multipolar)

How can we study neuronal morphology?

What are the basic principles and applications of **neuroanatomical techniques**?

https://www.jove.com/science-education/5204/an-introduction-to-neuroanatomy

Questions on neuroanatomical techniques

1. **Who was the first person to publish a description of brain anatomy?**

A) Wilder Penfield

B) Korbinian Brodman

C) Thomas Willis

D) Andreas Vesalius

2. **Who developed a staining technique to visualize single neurons and in what year?**

A) Korbinian Brodman in 1909

B) Camillo Golgi in 1873

C) Andres Vesalius in 1906

D) Santiago Ramón y Cajal in 1888

4. **Which of the following terms most appropriately refers to the microscopic arrangement of neurons?**

A) Neurogenetics

B) Cytoarchitecture

C) Neuroplasticity

D) Neurodegeneration

3.

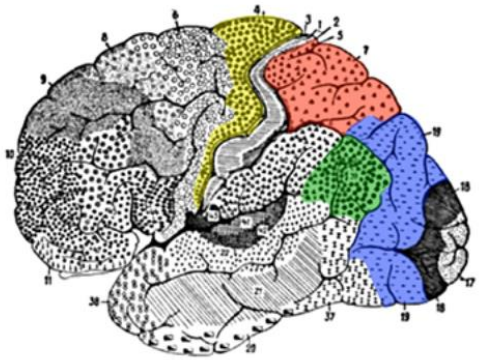

Figure 1 - Map of the Human Brain

In <u>Figure 1</u>, how were the various highlighted regions of the brain first distinguished from each other?

A) By their unique cellular architecture.

B) By their different motor functions.

C) By their different sensory functions.

D) By their sensitivity to neural stains.

5.

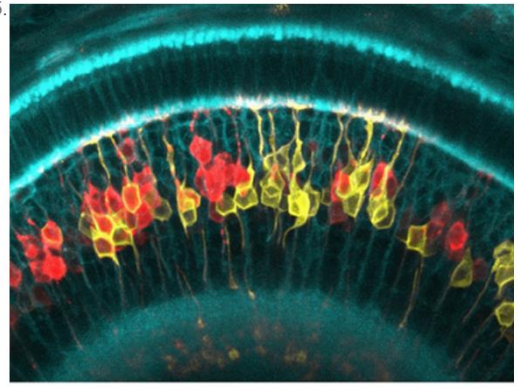

Figure 3 - Different Neurons Stained by Different Tracers

Which methodology made it possible to capture the image in <u>Figure 3</u>?

A) The Golgi stain

B) Dye injection

C) Fluorescence microscopy

D) Magnetic resonance imaging

6.

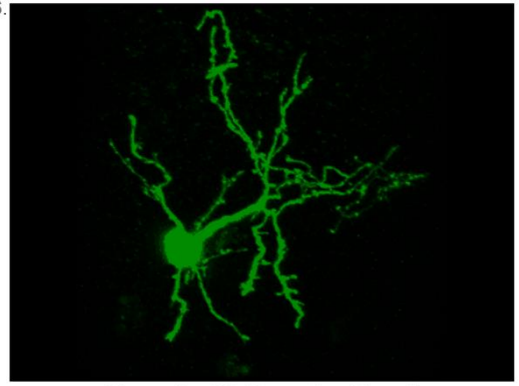

Figure 4 - 3D Reconstruction of Fluorescently Labeled Neuron

_____ microscopy allows for the creation of images seen in <u>Figure 4</u>.

A) Confocal

B) 2-Photon

C) Fluorescence

D) Electron

7.

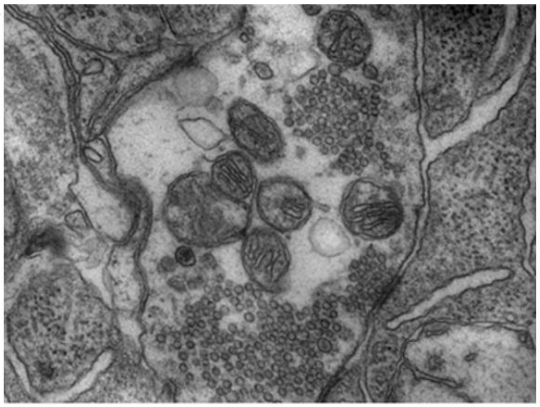

Figure 5 - Organelles in a Synaptic Terminal

The image in <u>Figure 5</u> was generated using _____ microscopy.

A) confocal

B) electron

C) 2-photon

D) atomic force

8. **Which of the following techniques is NOT a potential application of stereotaxic surgery?**

A) Injection of drugs

B) Generation of lesions

C) Neuronal cell culture

D) Delivery of electrical stimulation

Studying structure

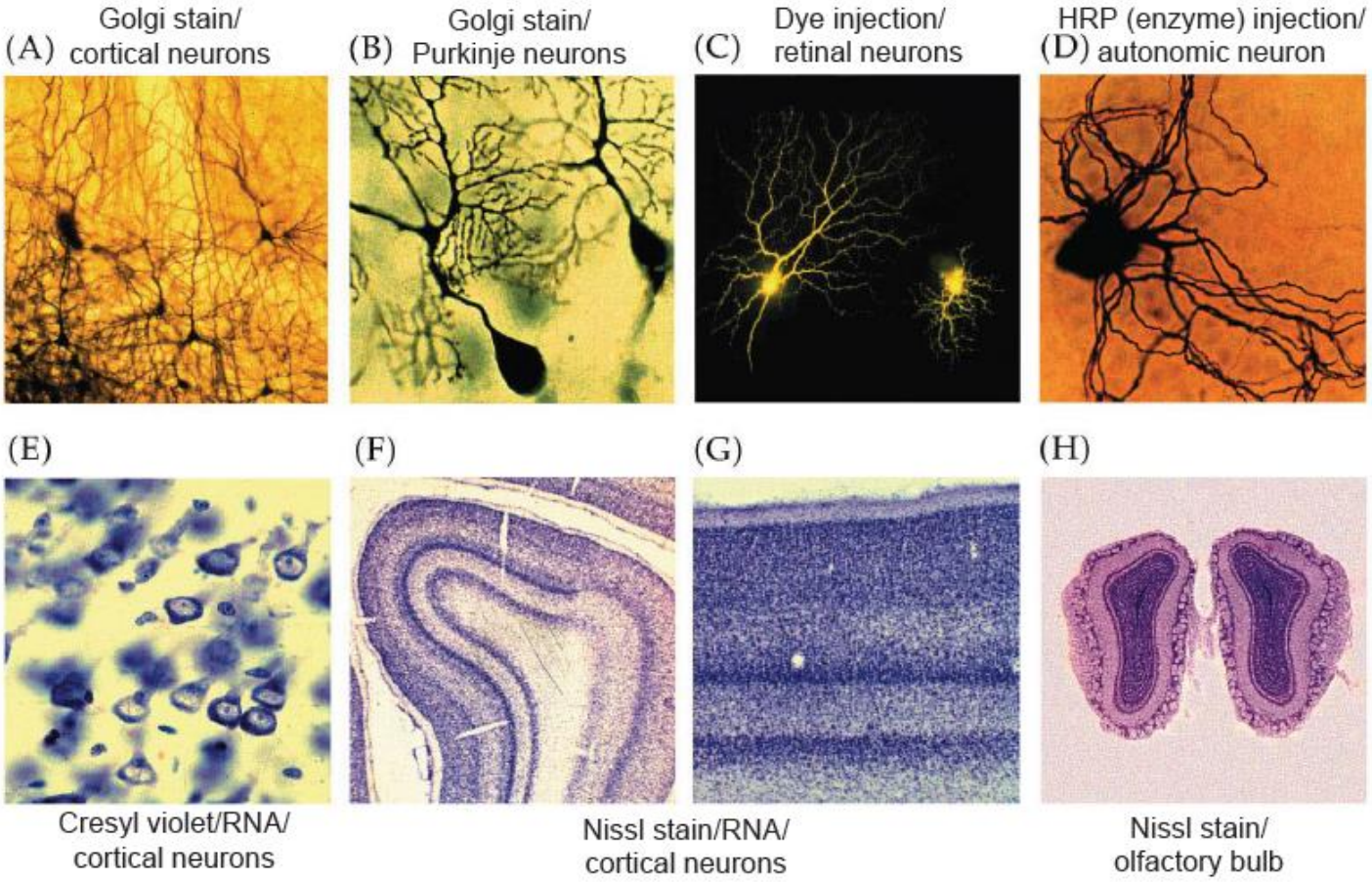

***NEUROSCIENCE, Fourth Edition,* Figure 1.6**

Which other types of neural staining can be used? For what purpose?

MOVIE

https://www.jove.com/science-education/5206/histological-staining-of-neural-tissue

Amazing diversification of neuronal shapes

- Multipolar neuron
  - most common
  - many dendrites/one axon
- Bipolar neuron
  - one dendrite/one axon
  - olfactory, retina, ear
- Unipolar neuron (pseudounipolar)
  - sensory from skin and organs to spinal cord
- Anaxonic neuron
  - many dendrites/no axon
  - help in visual processes

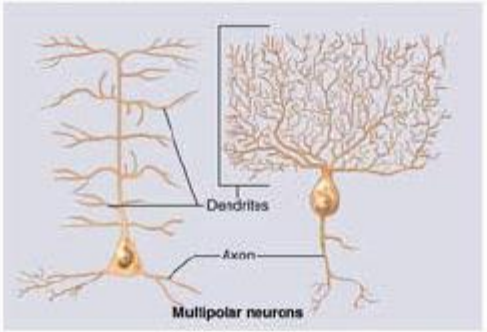

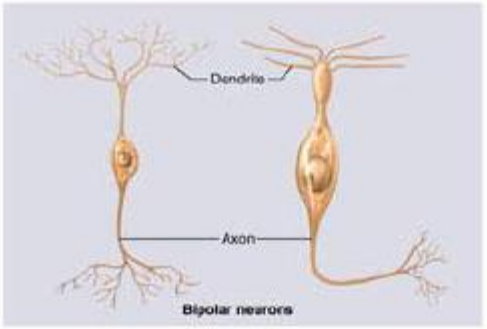

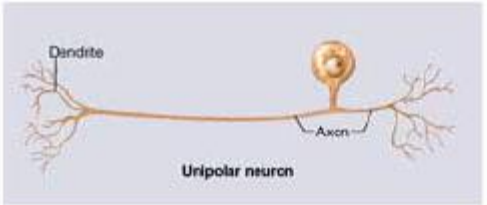

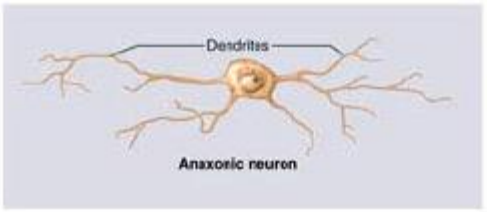

Morphology of vertebrate multipolar neurons is highly variable

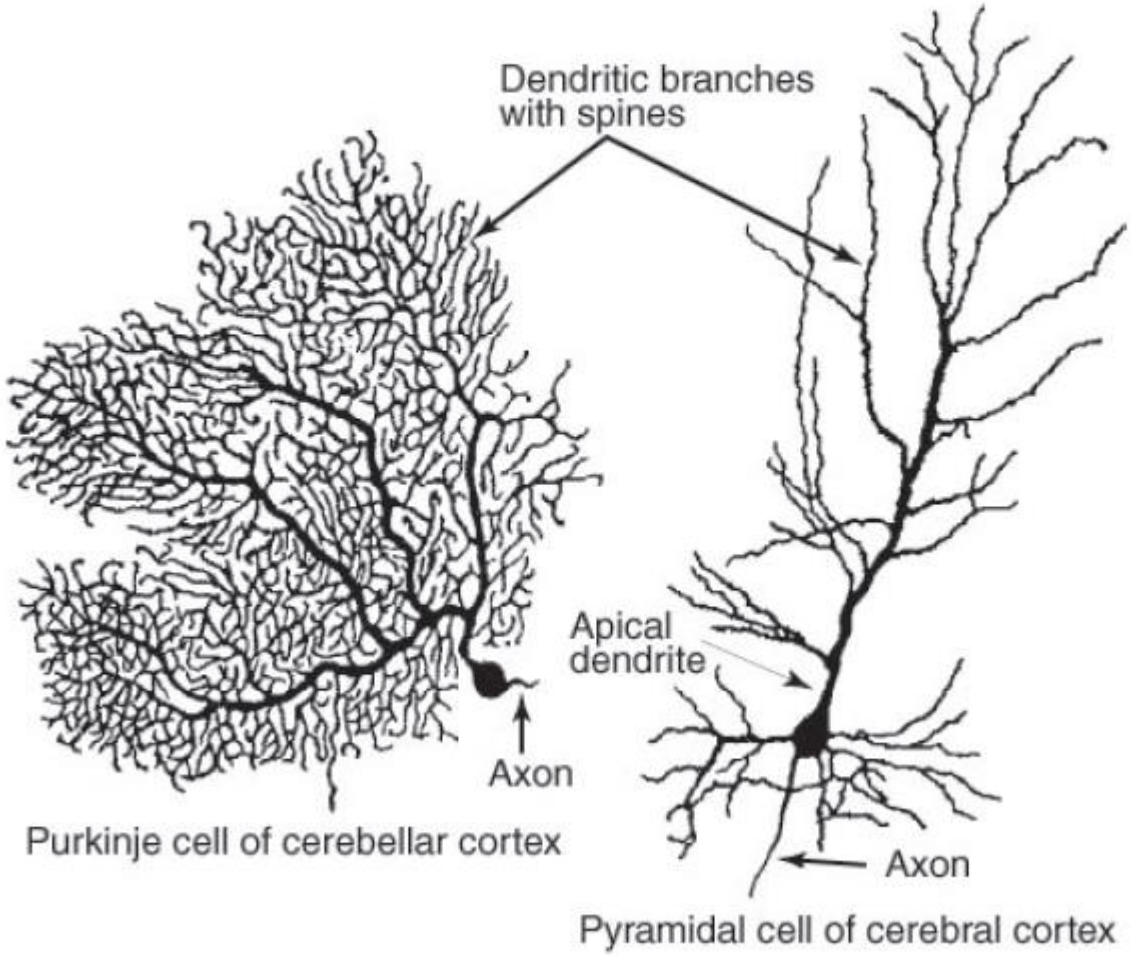

Fiala & Harris, 1999
Dendrite structure; in "Dendrites", Oxford Univ Press

Differences in arbor density reflect differences in connectivity

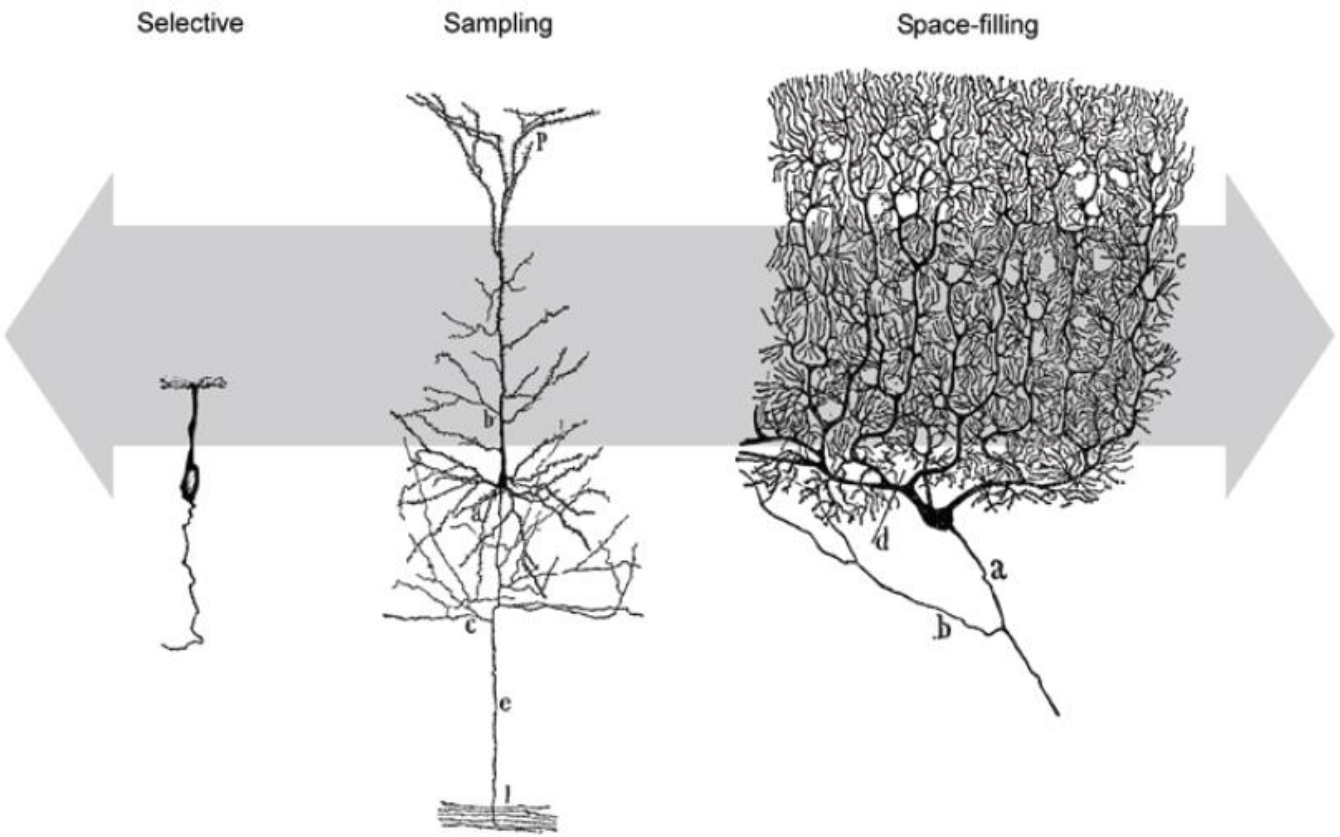

Fig. 1.5 The densities of dendritic arbors lie on a continuum of values. Differences in arbor density reflect differences in connectivity. At one extreme are selective arborizations in which each dendrite connects the cell body to a single remote target. An olfactory sensory cell is used to illustrate this. At the other extreme lie space-filling arborizations in which the dendrites cover a region, as with the cerebellar Purkinje cell. Intermediate arbor densities are referred to as sampling arborizations, as demonstrated by a pyramidal cell from cerebral cortex. (Drawings of neurons from Ramón y Cajal, 1995.)

Characteristic arborization patterns

Pattern	Characteristics	Examples
Adendritic 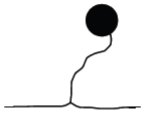	Cell body lacks dendrites	Dorsal root ganglion cells Sympathetic ganglion cells
Spindle radiation 	Two dendrites emerge from opposite poles of the cell body and have few branches	Lugaro cells Bipolar cells of cortex
Spherical radiation Stellate 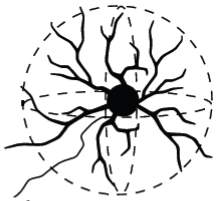	Dendrites radiate in all directions from cell body	Spinal neurons Neurons of subcortical nuclei (e.g. inferior olive, pons, thalamus, striatum) Cerebellar granule cells
Partial 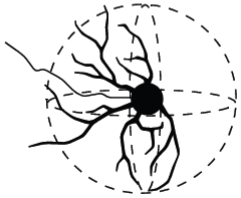	Dendrites radiate from cell body in directions restricted to a part of a sphere	Neurons at edges of "closed" nuclei (e.g. Clarke's column, inferior olive, vestibular nuclei)
Laminar radiation Planar 	Dendrites radiate from cell body in all directions within a thin domain	Retinal horizontal cells
Offset 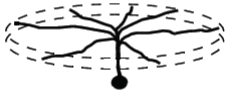	Plane of radial dendrites offset from cell body by one or more stems	Retinal ganglion cells
Multi 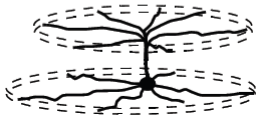	Cell has multiple layers of radial dendrites	Retinal amacrine cells

Fiala & Harris, 1999
Dendrite structure; in "Dendrites", Oxford Univ Press

Characteristic arborization patterns

Pattern	Characteristics	Examples
Cylindrical radiation 	Dendrites ramify from a central soma or dendrite in a thick cylindrical (disk-shaped) domain	Pallidal neurons Reticular neurons
Conical radiation 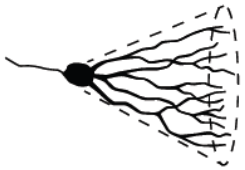	Dendrites radiate from cell body or apical stem within a cone or paraboloid	Granule cells of dentate gyrus and olfactory bulb Primary dendrites of mitral cells of olfactory bulb Semilunar cells of piriform cortex
Biconical radiation 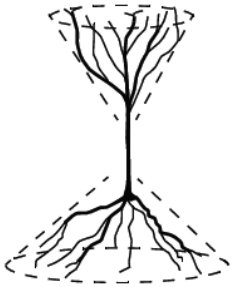	Dendrites radiate in opposite directions from the cell body	Bitufted, double bouquet, and pyramidal cells of cerebral cortex Vertical cells of superior colliculus
Fan radiation 	One or a few dendrites radiate from cell body in a flat fan shape	Cerebellar Purkinje cells

What changes among the dendrites ?

Table 1.1 Typical dimensions of dendrites for a few types of neurons

Neuron	Average soma diameter (μm)	Number of dendrites at soma	Proximal dendrite diameter (μm)	Number of branch points	Distal dendrite diameter (μm)	Dendrite extent* (μm)	Total dendritic length (μm)
Cerebellar granule cell (cat)	7	4	1	0	0.2-2	15	60
Starburst amacrine cell (rhesus)	9	1	1	40	0.2-2	120	—
Dentate gyrus granule cell (rat)	14	2	3	14	0.5-1	300	3200
CA1 pyramidal cell (rat)	21						11 900
basal dendrites		5	1	30	0.5-1	130	5500
stratum radiatum		1	3	30	0.25-1	110	4100
stratum lacunosum-moleculare				15	0.25-1	500	2300
Cerebellar Purkinje cell (guinea pig)	25	1	3	440	0.8-2.2	200	9100
Principal cell of globus pallidus (human)	33	4	4	12	0.3-0.5	1000	7600
Meynert cell of visual cortex (macaque)	35						15 400
basal dendrites		5	3	—	—	250	10 200
apical dendrites		1	4	15	2-3	1800	5200
Spinal a-motoneuron (cat)	58	11	8	120	0.5-1.5	1100	52 000

* The average distance from the cell body to the tips of the longest dendrites.

Sources: Ito (1984); Mariani (1990); Claiborne et al. (1990); Bannister and Larkman (1995a); Rapp et al. (1994); Palay (1978); Yelnik et al. (1984); Ulfhake and Kellerth (1981)

Fiala & Harris, 1999 Dendrite structure; in “Dendrites”, Oxford Univ Press

Methods for measuring dendritic complexity

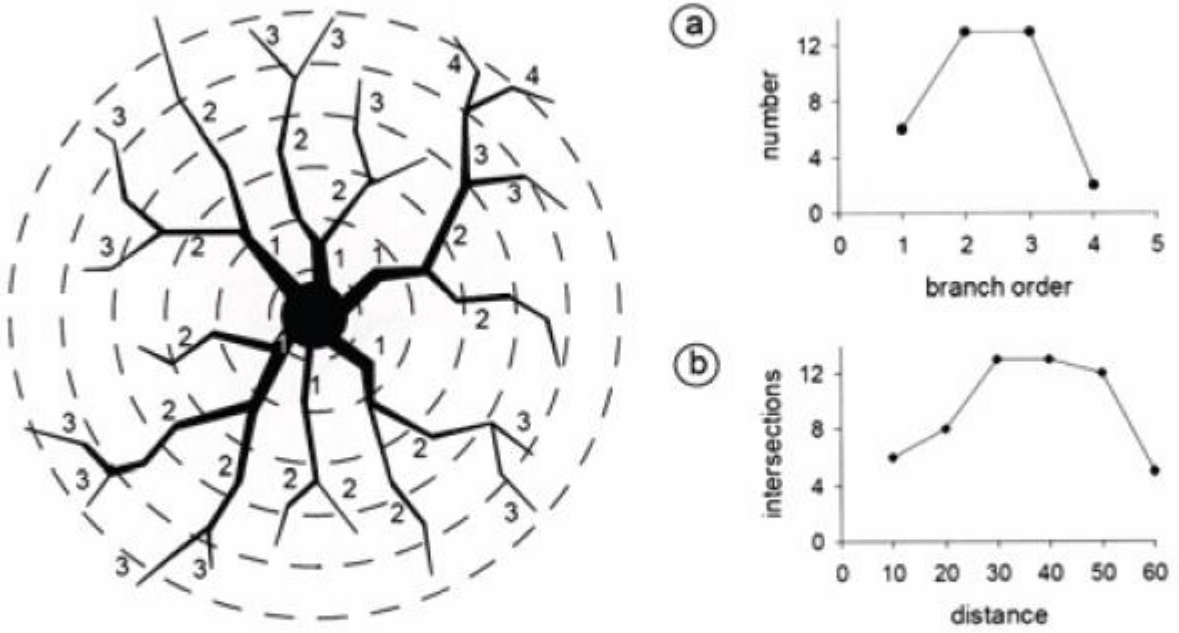

Fig. 1.4 Methods for characterizing dendritic branching. **(a)** A plot of the number of branches of each order using the centrifugal method of branch ordering. The *Strahler method* is similar but the dendritic tips are order 1 and branch numbers increase sequentially toward the soma. **(b)** A *Sholl plot* showing the number of intersections of the dendritic tree with circles of increasing radius from the center of the dendritic arbor. When three-dimensional data are available, concentric spheres are used rather than these circles centered on a two-dimensional projection of the neuron.

“Simple” neuronal classification separately considers morphology and basic functional features

Structural classification:

Unipolar, bipolar, multipolar (different arborization patterns) …

Functional classification:

- projection (inter)neurons
- local circuit (inter)neurons

- excytatory (neurotransmitters: Glutamate, etc.)
- inhibitory (neurotransm.: GABA, glycine, etc.)

Two fundamental types of neurons in cerebral cortex:

- projection (**Pyramidal**) neurons
- local circuit neurons (**Interneurons**)

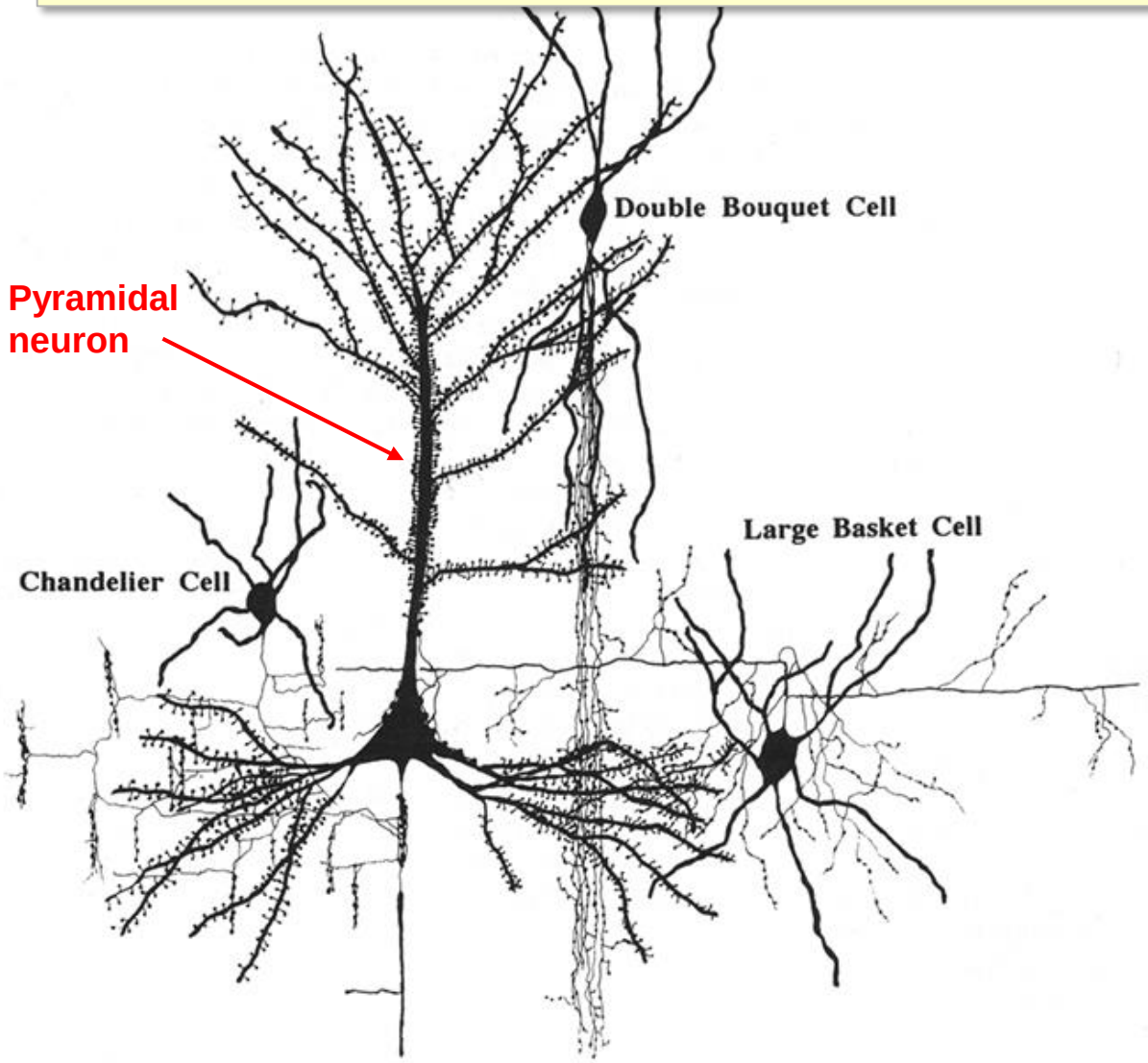

GABAergic interneurons comprise 20–30% of the cortical neuronal population and are locally projecting cells that control and synchronize the output of **pyramidal** neurons.

Interestingly, the influence of GABAergic interneurons on pyramidal cells is largely dependent on the subcellular location of their inputs, which varies among different interneuron subtypes.

A key feature of **cortical inhibitory interneurons** is the structural and functional diversity

How many subtypes of interneurons exists?

How can we classify them?

How can we put together information from different approaches?

Different classification approaches of cortical interneurons

Morphologically defined subtypes of interneurons

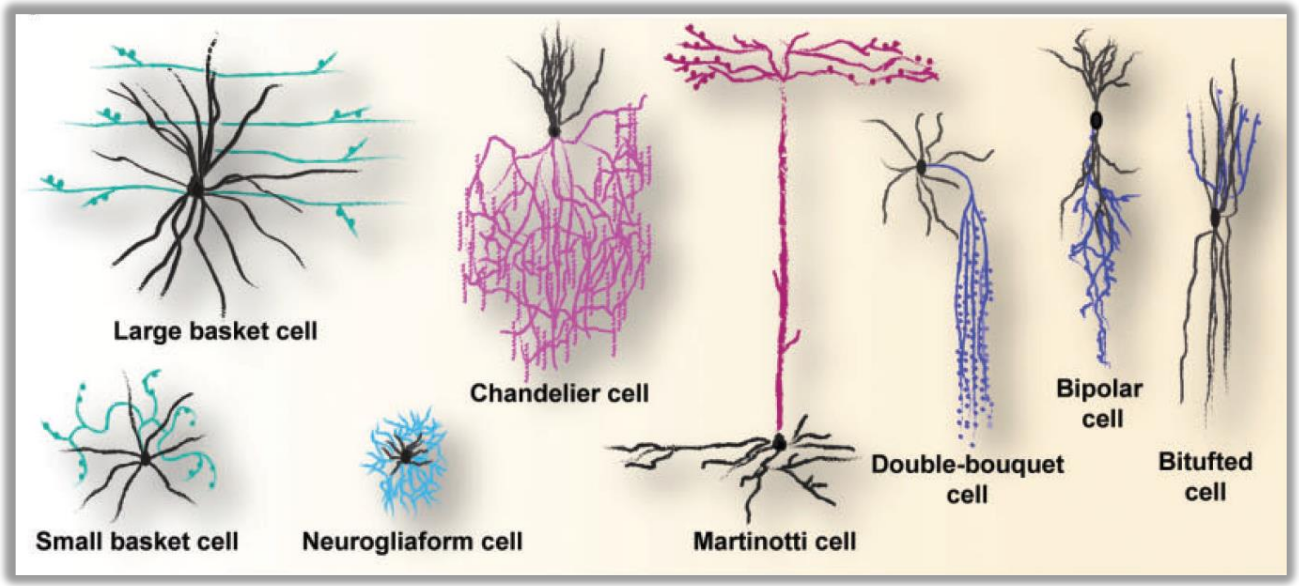

Black and colored lines represent dendritic and axonal processes, respectively

Electrophysiological classification

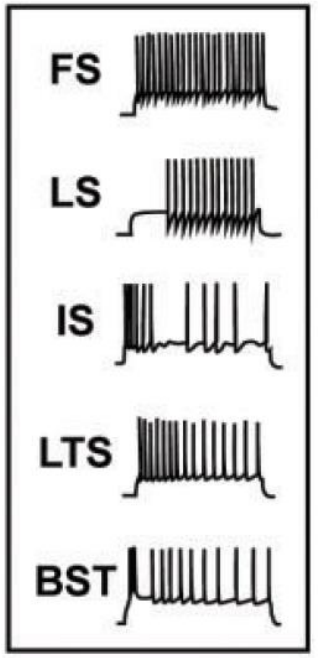

based on the action potential response pattern upon electrical stimulation.
FS, fast-spiking; LS, late-spiking; IS, irregular-spiking; LTS, low threshold spiking; BST, bursting

Sultan & Shi, 2018

WIREs Dev Biol 2018, 7:e306. doi: 10.1002/wdev.306

Diversity in subcellular targeting

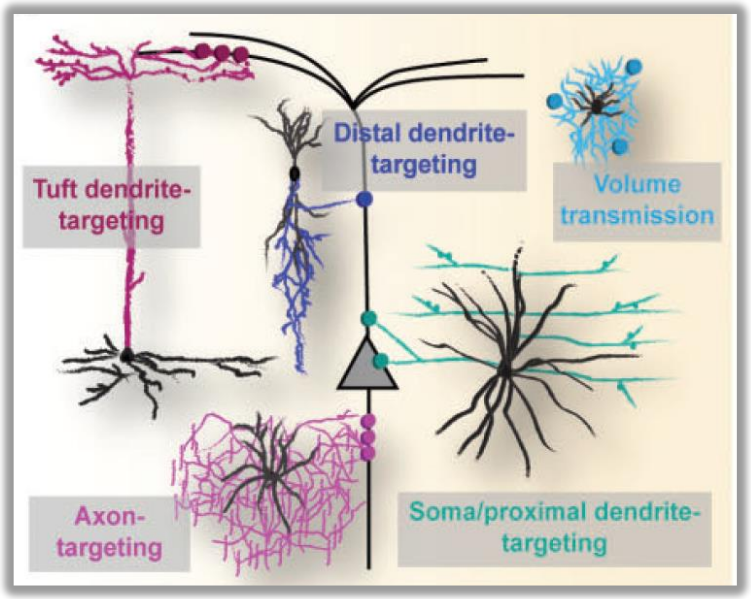

Classification of subtypes based on molecular marker expression

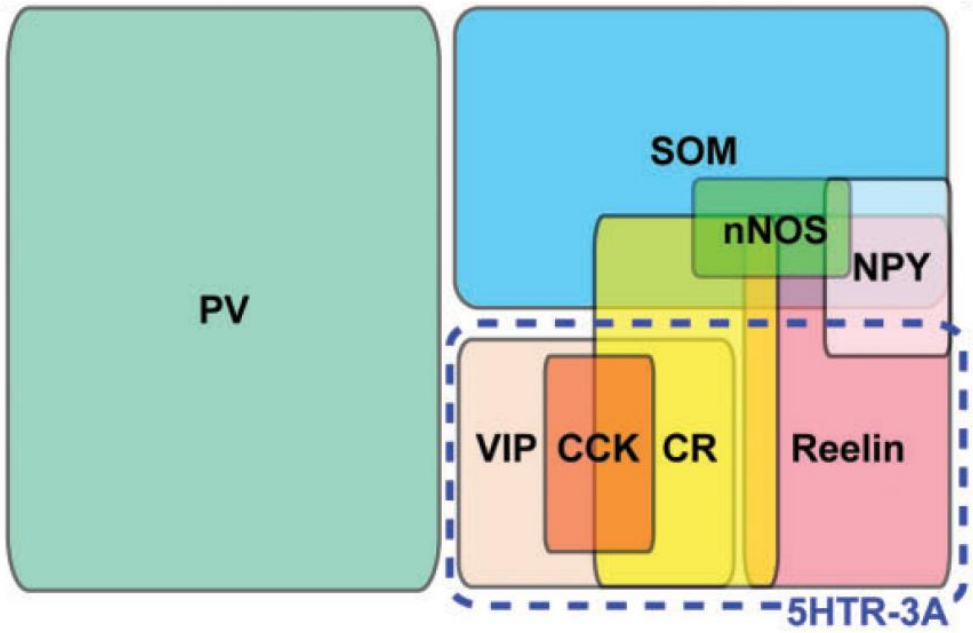

PV, parvalbumin; SOM, somatostatin; VIP, vasointestinal peptide; CR, calretinin; CCK, cholecystokinin; NPY, neuropeptide Y; 5HTR-3A, serotonin receptor 3A.

Sultan & Shi, 2018

WIREs Dev Biol 2018, 7:e306. doi: 10.1002/wdev.306

COMBINING different approaches to define INTERNEURON SUBTYPES.

Localization of Calcium-binding Proteins in Physiologically and Morphologically Characterized Interneurons of Monkey Dorsolateral Prefrontal Cortex

A.V. Zaitsev[1], G. Gonzalez-Burgos[1], N.V. Povysheva[1], S. Kröner[2,3], D.A. Lewis[1,2] and L.S. Krimer[1]

Cerebral Cortex August 2005;15:1178-1186

(1) Whole-cell electrophysiological recording on cortical slices

+

(2) intracellular injection of byocytin in recorded neurons (for later recognition and morphological analysis)

+

(3) fluorescence immunocytochemistry for selected markers (calcium-binding proteins: parvalbumin, calbindin and calretinin)

ABSTRACT

In the primate neocortex, little is known about the possible associations between functional subclasses of GABA neurons, their morphological properties and calcium-binding protein (CaBP) content. We used whole-cell current clamp recordings, combined with intracellular labeling and fluorescence immunohistochemistry, to determine these relationships for interneurons in layers 2–3 of monkey prefrontal cortex (PFC). Eighty-one interneurons were included in the analysis. Thirty-eight of these cells showed immunoreactivity for one of the three CaBPs tested. Co-localization of more than one CaBP was not observed in any of the interneurons examined. Interneurons with different CaBPs formed distinct populations with specific physiological membrane properties and morphological features. Parvalbumin (PV)-positive cells had the physiological properties characteristic of fast-spiking interneurons (FS) and the morphology of basket or chandelier neurons. Most calretinin (CR)-containing cells had the physiological properties ascribed to non-fast-spiking cells (non-FS) and a vertically oriented axonal morphology, similar to that of double bouquet cells. Calbindin (CB)-positive interneurons also had non-FS properties and included cells with double bouquet morphology or with a characteristic dense web of axonal collaterals in layer 1. Classification of the interneurons based on cluster analysis of multiple electrophysiological properties suggested the existence of at least two distinct groups of interneurons. The first group contained mainly PV-positive FS cells and the second group consisted predominantly of CR- and CB-positive non-FS interneurons. These findings may help to illuminate the functional roles of different groups of interneurons in primate PFC circuitry.

The phenotype of BC-injected/electrophysiologically-recorded interneurons is determined by immunocytochemistry

Zaitsev et al., 2005
Cerebral Cortex
doi:10.1093/cercor/bhh218

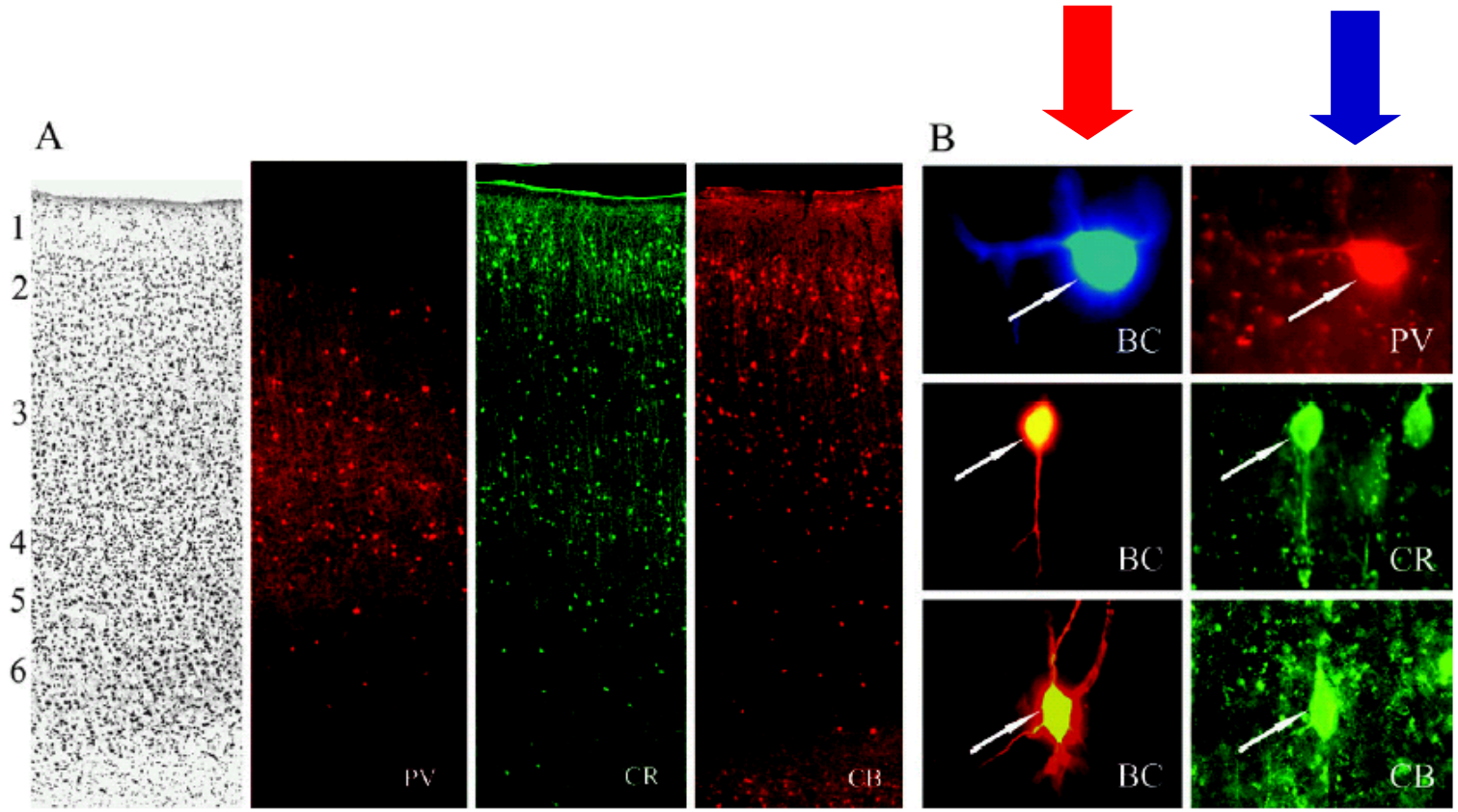

Figure 1. Fluorescence-labeling of CaBPs in monkey DLPFC interneurons. (A) Photomicrographs of adjacent coronal sections (area 46) with laminar boundaries; from left Nissl stain, PV-, CR- and CB-IR structures. Note the substantial differences in the laminar distribution of the neurons labeled for each CaBP. (B) Dual-label photomicrographs from the same microscopic field, showing immunohistochemical identification of physiologically characterized biocytin (BC)-injected interneurons as positive for PV, CR or CB. Arrows show the cell bodies. Top: BC visualized by streptavidin-Alexa FluorÒ 350 conjugate (blue), PV-IR visualized by Alexa FluorÒ 594 conjugated secondary antibody. Middle: BC visualized by streptavidin-Alexa FluorÒ 568 conjugate, CR-IR visualized by Alexa FluorÒ 488 conjugated secondary antibody. Bottom: BC visualized by streptavidin-Alexa FluorÒ 568 conjugate, CB-IR visualized by Alexa FluorÒ 488 conjugated secondary antibody.

https://www.jove.com/science-education/5040/introduction-to-fluorescence-microscopy

The combination of intracellular-injection techniques and immunocytochemistry suggests that the same phenotypic marker is expressed by interneurons with different morphologies

Do different morphologies indicate different functional features?

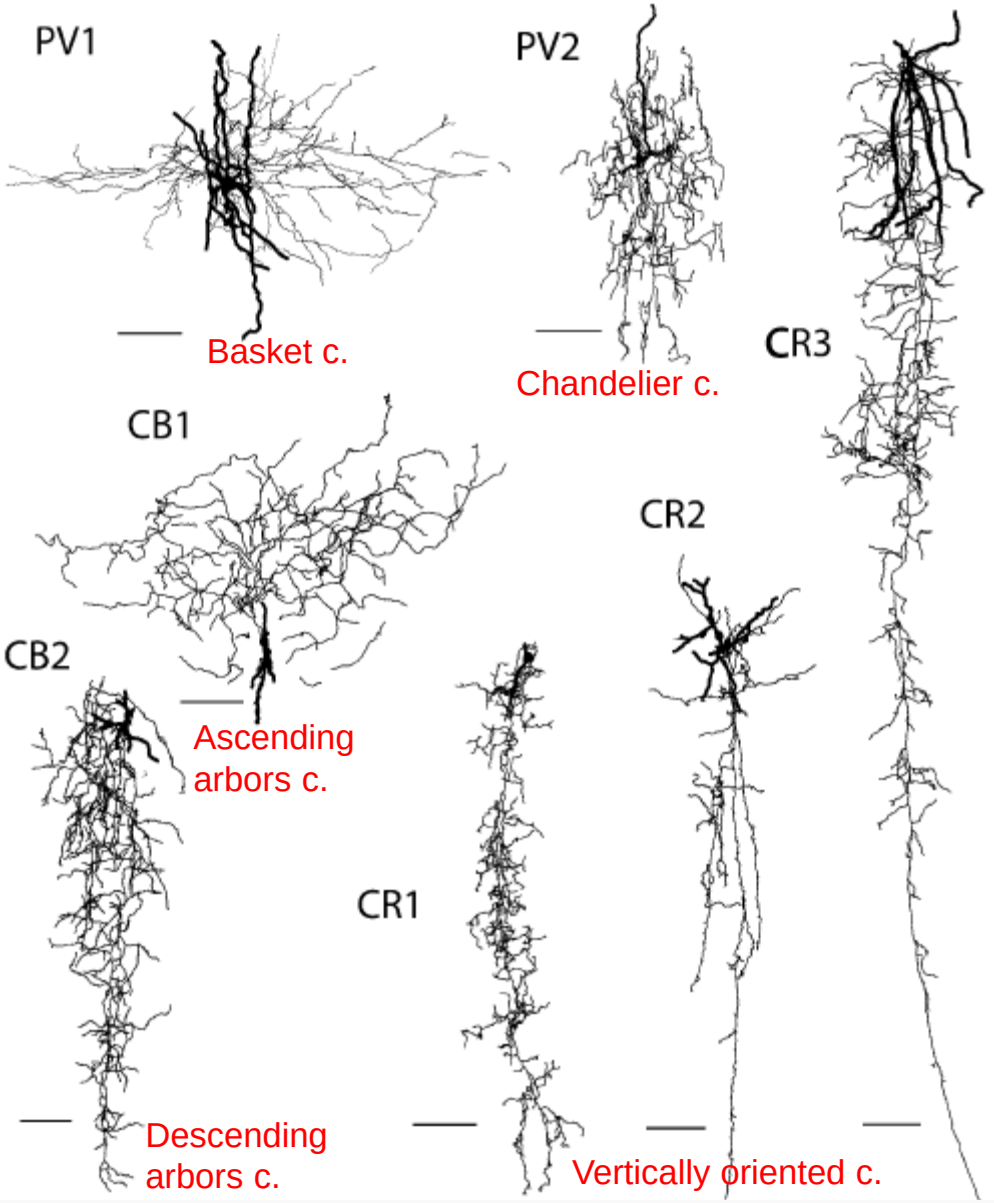

Figure 2. Three-dimensional reconstructions of biocytin-labeled interneurons from monkey DLPFC. PV1, PV-IR spreading arbor (basket) cell; PV2, PV-IR chandelier cell; CR1-CR3, examples of CR-IR vertically oriented cells; CB1, CB-IR cell with ascending arbors; CB2, CB-IR cell with descending arbors. Calibration bars = 100 μm.

Zaitsev et al., 2005
Cerebral Cortex
doi:10.1093/cercor/bhh218

Data were processed using **CLUSTER ANALYSIS:** correlation between **electrophysiological properties** and **expression of specific Ca^{+}-binding proteins**

When cells are grouped based only on electrophysiological properties, two main groups (= clusters) of interneurons are obtained: FS (Fast Spiking) and non-FS.

These two clusters do show significant differences in Ca^{+}-binding protein content

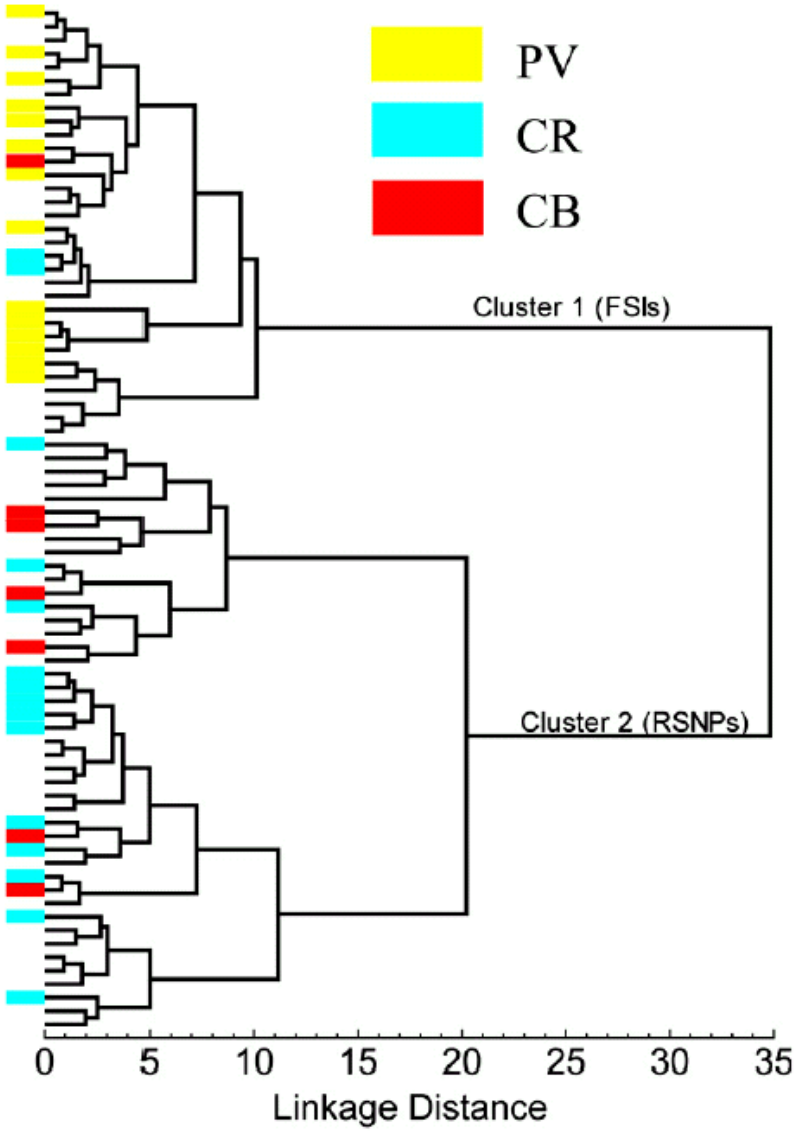

Figure 4. Hierarchical tree plot illustrating the results of cluster analysis. There are two main branches corresponding to FS interneurons (FSI) and non-FS cells. The first cluster mainly contained PV-positive interneurons and the second one consisted exclusively of CB- and CR-positive cells.

Zaitsev et al., 2005
Cerebral Cortex
doi:10.1093/cercor/bhh218

CONCLUSIONS:

- parvalbumin-expressing interneurons are exclusively FS
- calretinin- and calbindin-expressing interneurons are mainly non-FS
- multiple morphologies can correspond to a single functionally-defined phenotype

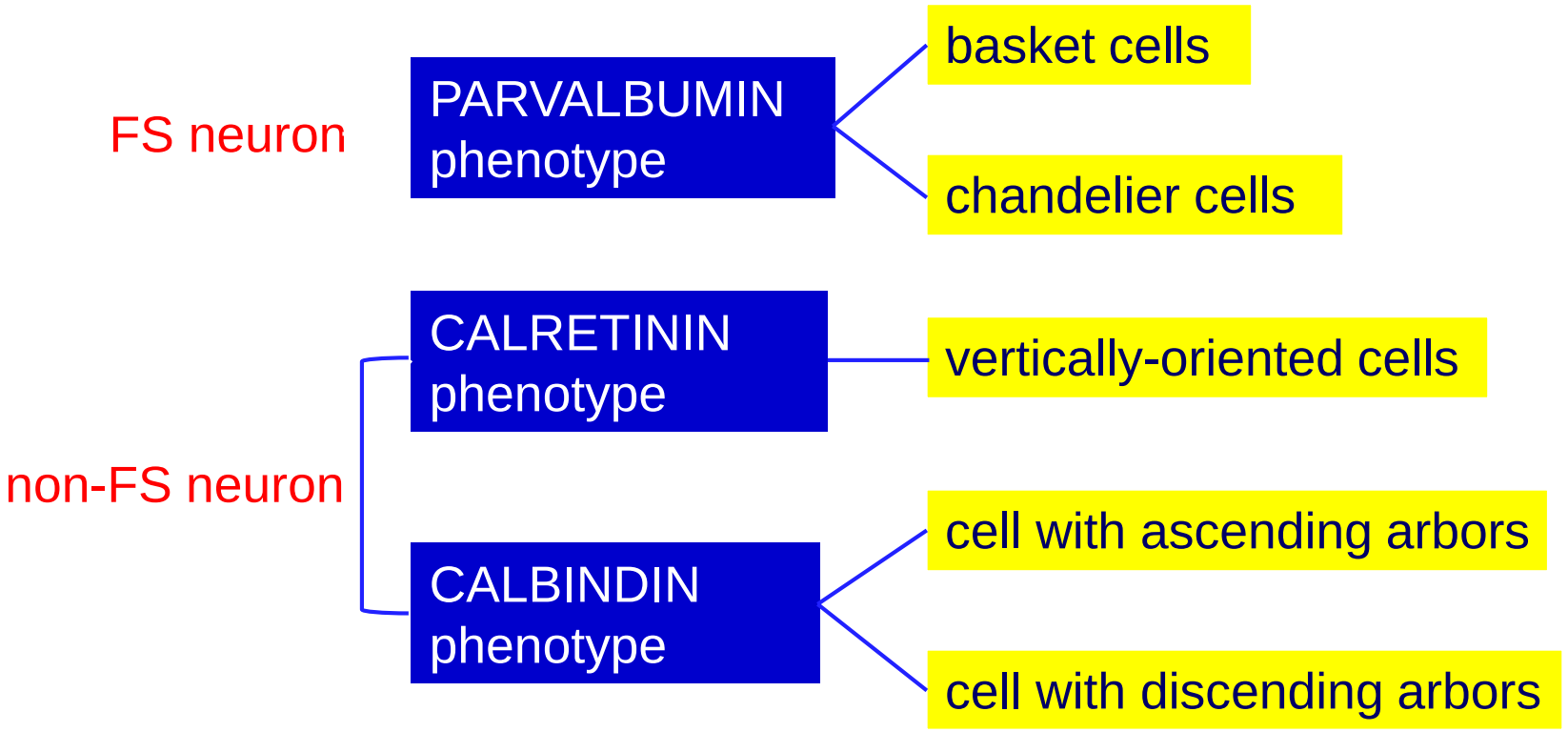

Electrophysiological and gene expression profiling of neuronal cell types

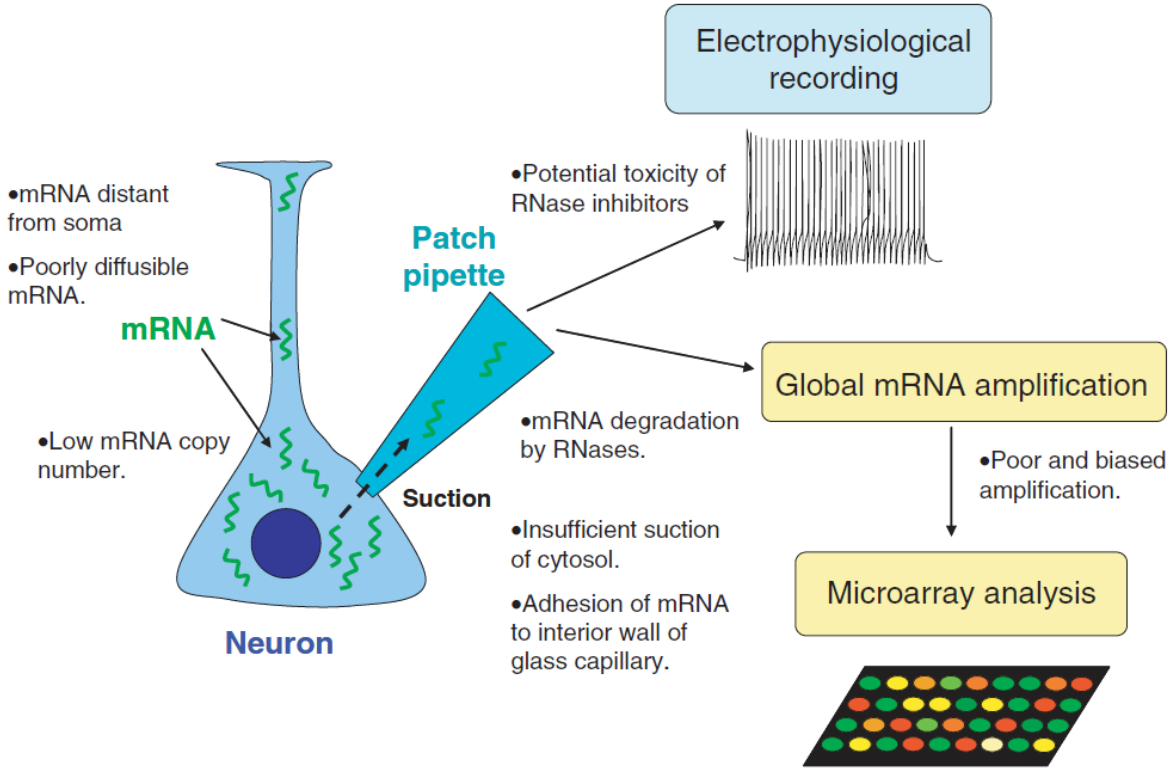

Figure 1. Potential problems with single-cell gene expression profiling by cytoplasmic harvesting via patch-pipette

Collecting extremely low amounts of mRNA from single cells is the biggest challenge of this technique. Only a small proportion of cytosol can be obtained by suction via patch-pipette, and poorly diffusible mRNA or dendritic mRNA are particularly hard to collect. The yield of mRNA can be improved by including inhibitors of RNases in the pipette, but these are often cytotoxic and can be detrimental to electrophysiological recording. It is also possible that some mRNA adheres to the interior wall of the glass capillary and evades expulsion from the patch-pipette.

Yano et al., 2006 J Physiol
DOI: 10.1113/jphysiol.2006.113712

Integration of electrophysiological recordings with single-cell RNA-seq data identifies neuronal subtypes

nature biotechnology

Fuzik et al., 2016
Nature Biotechnology
doi:10.1038/nbt.3443

János Fuzik[1,2,5], Amit Zeisel[1,5], Zoltán Máté[3], Daniela Calvigioni[1,2], Yuchio Yanagawa[4], Gábor Szabó[3], Sten Linnarsson[1,6] & Tibor Harkany[1,2,6]

Traditionally, neuroscientists have defined the identity of neurons by the cells' location, morphology, connectivity and excitability. However, the direct relationship between these parameters and the molecular phenotypes has remained largely unexplored. Here, we present a method for obtaining full transcriptome data from single neocortical pyramidal cells and interneurons after whole-cell patch-clamp recordings in mouse brain slices. In our approach, termed Patch-seq, a patch-clamp stimulus protocol is followed by the aspiration of the entire somatic compartment into the recording pipette, reverse transcription of RNA including addition of unique molecular identifiers, cDNA amplification, Illumina library preparation and sequencing. We show that Patch-seq reveals a close link between electrophysiological characteristics, responses to acute chemical challenges and RNA expression of neurotransmitter receptors and channels. Moreover, it distinguishes neuronal subpopulations that correspond to both well-established and, to our knowledge, hitherto undescribed neuronal subtypes. Our findings demonstrate the ability of Patch-seq to precisely map neuronal subtypes and predict their network contributions in the brain.

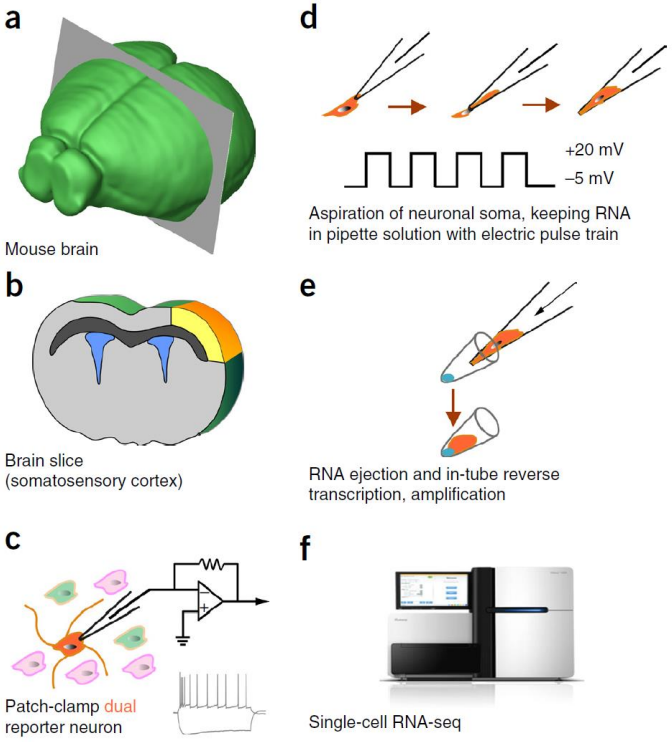

A new way to identify neuronal subtypes with transcriptomics: Patch-seq = patch-clamp + Next Generation Sequencing

focusing on cholecystokinin (CCK)-containing(+) GABAergic interneurons by using **dual-labeled CCKBAC/dsRed::GAD67gfp/+ mouse reporter**

Figure 2 Workflow diagram of Patch-seq procedures. (**a**) Coronal cutting plane of a mouse brain to access the somatosensory cortex. (**b**) *Ex vivo* brain slice anatomy with the somatosensory cortex highlighted in yellow and orange. (**c**) Whole-cell patch-clamp recording of DsRed^{+}/GFP^{+} dual-tagged interneurons. (**d**) Aspiration of neuronal somata was followed by square voltage pulses from –5 mV (holding potential) to +20 mV, while maintaining negative pressure. (**e**) The sample was expelled into lysis buffer, which allowed for in-tube reverse transcription by PCR. (**f**) Single-cell RNA sequencing performed on an Illumina Hiseq2000 instrument.

NATURE NEUROSCIENCE VOLUME 19 | NUMBER 2 | FEBRUARY 2016

Adult mouse cortical cell taxonomy revealed by single cell transcriptomics

Bosiljka Tasic[1,2], Vilas Menon[1,2], Thuc Nghi Nguyen[1], Tae Kyung Kim[1], Tim Jarsky[1], Zizhen Yao[1], Boaz Levi[1], Lucas T Gray[1], Staci A Sorensen[1], Tim Dolbeare[1], Darren Bertagnolli[1], Jeff Goldy[1], Nadiya Shapovalova[1], Sheana Parry[1], Changkyu Lee[1], Kimberly Smith[1], Amy Bernard[1], Linda Madisen[1], Susan M Sunkin[1], Michael Hawrylycz[1], Christof Koch[1] & Hongkui Zeng[1]

The most complete single-neuron transcriptome database of the mouse visual cortex was performed using a large collection of reporter mouse lines. Results highlight the unmatched neuronal diversity of the cerebral cortex.

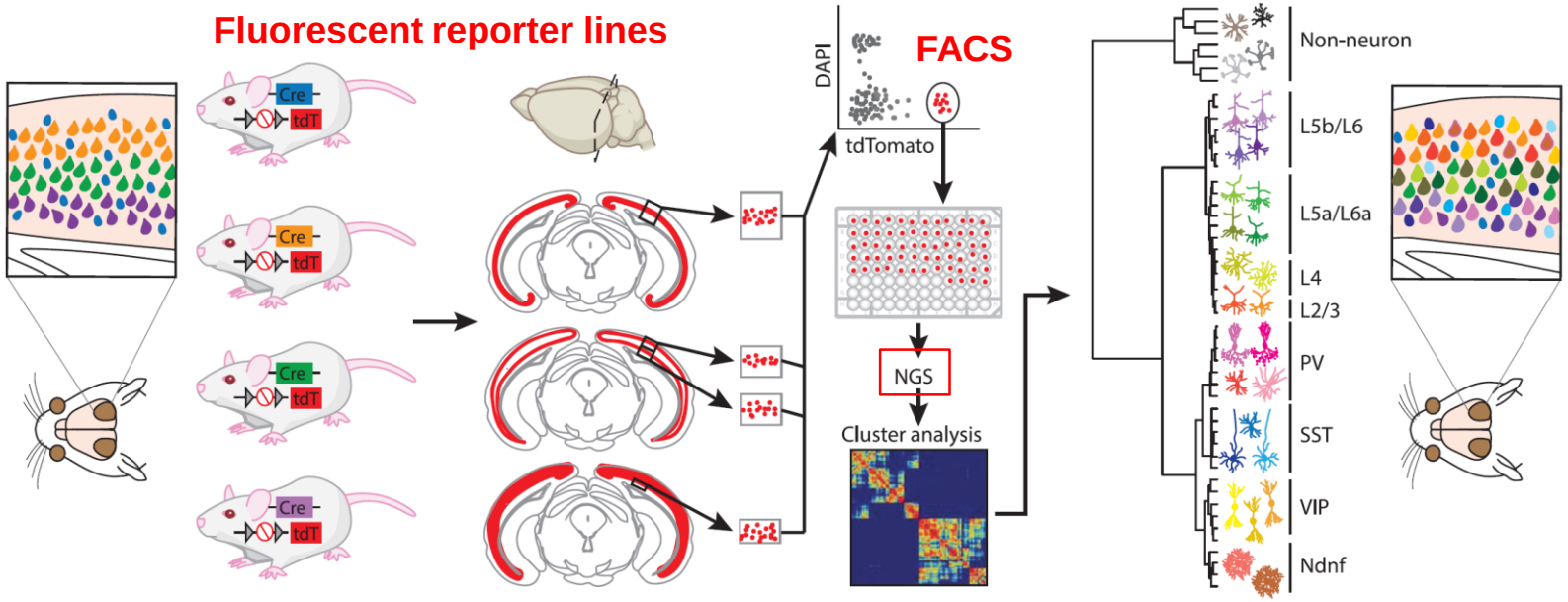

Figure 1 Single-neuron RNA-seq analysis of the adult mouse visual cortex. A large repertoire of Cre driver lines crossed to *loxP* tdTomato (tdT) reporter lines was used to label distinct neuronal populations in the mouse visual cortex. Specific layers of the primary visual cortex were microdissected from freshly sectioned adult mouse brains, and single neurons from these samples were purified by fluorescence-activated cell sorting for use in single-cell RNA-seq. Cluster analysis was conducted agnostic to the reporter line of origin. The resulting clusters were assigned to 49 transcriptionally defined cell types, 42 of them neuronal, highlighting the molecular diversity in classes of cortical excitatory and inhibitory neurons. PV, parvalbumin; SST, somatostatin; VIP, vasoactive intestinal polypeptide; Ndnf, neuron derived neurotrophic factor; NGS, next generation sequencing.

http://casestudies.brain-map.org/celltax#section_introa

The Allen Brain Atlas cell taxonomy project